MOL # 57513

Simple 2,4 diacylphloroglucinols as TRPC6 activators – identification of a novel pharmacophore.

Leuner K.[*], Heiser J.H.[*], Derksen S., Mladenov M. I., Fehske C.J, Schubert R, Gollasch M., Schneider G., Harteneck C., Chatterjee S.S., Müller W.E.

Institute of Pharmacology, Biocenter Niederursel, Goethe University, Max-von-Laue-Str. 9, 60439 Frankfurt am Main, Germany; KL, JHH, CJF, WEM
Beilstein Endowed Chair for Cheminformatics, Institute for organic chemistry and chemical biology, Siesmayerstr. 70, 60323 Frankfurt am Main, Germany; SD,GS
Cardiovascular Physiology, Centre for Biomedicine and Medical Technology Mannheim, Ruprecht-Karls-University Heidelberg, Ludolf-Krehl-Str. 13-17, 68167 Mannheim, Germany; MIM, RS
Institute of Biology, Faculty of Natural Sciences and Mathematics, 'Sts. Cyril and Methodius', University of Skopje, Skopje, Macedonia; MIM
Charité University Medicine, Section Nephrology/Intensive Care, Campus Virchow, and Experimental and Clinical Research Center (ECRC), Augustenburger Platz 1, 13353 Berlin, Germany; MG
Molecular Pharmacology and Cell Biology, Charité, 14195 Berlin & Institute of Pharmacology and Toxicology & Interfaculty Centre for Pharmacogenomics and Drug Research (ICePha), Eberhard-Karls-University, Wilhelmstr. 56, 72074 Tübingen, Germany; CH
Dr. Willmar Schwabe GmbH & Co.KG Pharmaceuticals, 76227 Karlsruhe, Germany; SSC

1

MOL # 57513

Running title: Acylphloroglucinol derivatives as TRPC6 activators

Corresponding authors:
Dr. Kristina Leuner
Institute of Pharmacology
Goethe University
Biocenter N260 1. Floor
Max-von-Laue-Str. 9
60438 Frankfurt
Germany
Tel.: +49-69-79829365
Fax: +49-69-79829374
Leuner@em.uni-frankfurt.de

PD Dr. Christian Harteneck
Institute of Pharmacology and Toxicology
Eberhard-Karls-University
Wilhelmstr. 56
72074 Tübingen
Germany

Text pages: 23
Figures: 8
Numbers of tables: 0
References: 26
Words in the abstract: 248
Words in the introduction: 724
Words in the discussion: 582

Non-standard abbreviations: DAG, diacylglycerol; DN, dominant negative; PIP_2, phosphatidylinositol-4,5-bisphosphate; PLC, phospholipase C; PUFA, poly-unsaturated fatty acid; TRPC, canonical transient receptor potential; TRPV, vanilloid-like; TRPM, melastatin-like; TRPP, polycystins; TRPML, mucolipidin; TRPA, ankyrine-rich; TRPN, nompC-like; YFP, yellow fluorescent protein

2

MOL # 57513

Abstract

The naturally occurring acylated phloroglucinol derivative hyperforin was recently identified as the first specific TRPC6 activator. Hyperforin is the major antidepressant component of St. John's wort, which mediates its antidepressant-like properties via TRPC6 channel activation. However, its pharmacophore moiety for activating TRPC6 channels is unknown. We hypothesised that the phloroglucinol moiety could be the essential pharmacophore of hyperforin and that its activity profile could be due to structural similarities with DAG, an endogenous nonselective activator of TRPC3, TRPC6, TRPC7. Accordingly, a few 2-acyl and 2,4-diacylphloroglucinols were tested for their hyperforin-like activity profiles. We used a battery of experimental models to investigate all functional aspects of TRPC6 activation, including ion channel recordings, Ca^{2+} imaging, neurite outgrowth, and inhibition of synaptosomal uptake. Phloroglucinol itself was inactive in all our assays, which was also the case for 2-acylphloroglucinols. For TRPC6 activation, the presence of two symmetrically acyl-substitutions with appropriate alkyl chains in the phloroglucinol moiety seem to be an essential prerequisite. Potencies of these compounds in all assays were comparable to that of hyperforin for activating the TRPC6 channel. Finally, using structure-based modelling techniques a binding mode for hyperforin to TRPC6 is suggested. Based on this modelling approach, we propose that DAG is able to activate all three TRPC3, TRPC6, TRPC7 due to higher flexibility within the chemical structure of DAG compared to the rather rigid structures of hyperforin, and the 2,4-diacylphloroglucinol derivatives.

MOL # 57513

Introduction

Hyperforin is the main active ingredient of St. John's wort, which is used for centuries to treat depression (Linde *et al.*, 2008). Like most synthetic antidepressants, hyperforin inhibits synaptic reuptake of serotonin and norepinephrine (Müller, 2003; Treiber *et al.*, 2005). Hyperforin is an acylated bicyclic phloroglucinol derivative with little structural and functional resemblances with any known therapeutically used antidepressants. Thus, unlike conventionally known antidepressants, hyperforin is not a competitive inhibitor of neurotransmitter transporters, and it inhibits synaptic neurotransmitter reuptake by elevating intracellular sodium concentrations (Singer *et al.*, 1999; Wonnemann *et al.*, 2000). Recent attempts to figure out its molecular target led us identify hyperforin as the first and highly selective activator of the TRPC6, a member of the TRP superfamily (Treiber *et al.*, 2005; Leuner *et al.*, 2007).

The TRP superfamily of cation channels encompasses 29 mammalian members. Based on sequence homology and functional data, they can be subdivided in the classic (TRPC), vanilloid-like (TRPV), melastatin-like (TRPM), polycystins (TRPP), mucolipidin (TRPML), ankyrine-rich (TRPA) and nompC-like (TRPN) TRP subfamilies (Montell, 2005; Voets *et al.*, 2005; Montell, 2006). TRP channels are homo- and heterotetramers of subunits containing six transmembrane segments (S1 – S6) and cytoplasmic N- and C-terminal tails. S5, S6 and the connecting pore loop form the cation-conducting pore. S1 – S4 and the cytoplasmic N- and C-terminals are important for channel gating and the interaction with ligands or proteins (Voets *et al.*, 2005; Voets and Nilius, 2007).

TRP channels are involved in a variety of physiological functions. The discovery of their role in temperature sensation and pain was accelerated by the observation that direct and selective activation of TRP channel isoforms underlies the effects of several secondary plant compounds to modulate temperature sensation and cause pain, such as capsaicin, menthol, cinnamaldehyde, gingerol, and campher (Mandadi and Roufogalis, 2008). TRPC6 is one member of the canonical TRP channel subfamily, which consists of seven members, TRPC1 – TRPC7 (Dietrich and Gudermann, 2007). TRPC channels are highly expressed in the brain and are activated by G-protein coupled receptors, or receptor tyrosine kinases such as mGluR1 or TrKB, which play important roles in

4

neuronal plasticity and memory functions (Jia *et al.*, 2007; Tai *et al.*, 2008; Zhou *et al.*, 2008). The primary mode of activation of TRPC channels in cell physiology is considered to be linked to phospholipase C (PLC) (Montell, 2005). PLC-mediated degradation of phosphatidylinositol-4,5-bisphosphate (PIP_2) results in the accumulation of diacylglycerol (DAG), which is considered to be the physiological activator of TRPC3, TRPC6- and TRPC7-mediated currents (Hofmann *et al.*, 1999; Trebak *et al.*, 2003; Dietrich and Gudermann, 2007). However, the binding site of DAG at the TRPC6 channel is yet to be identified. Furthermore, several contradicting concepts regarding the activation mechanism of TRPC6 are discussed. The groups around Lemonnier et al. and Jardin et al. reported a significant and pronounced activation of TRPC6 by PIP_2, whereas Kwon et al. showed a disruption of TRPC6 activity by PIP_2 and propose that PIP_2 metabolites such as PIP_3 directly binds to TRPC6 channels and interferes with the calmodulin binding site at the C-terminus (Lemonnier *et al.*, 2008; Jardin *et al.*, 2008; Kwon *et al.*, 2007). The situation became more complex by several reports describing the PIP_2-dependent modulation of TRP channels [for review see (Voets and Nilius, 2007)]. In the case of TRPV1, Brauchi et al. (2007) calculated a homology model with the proposed PIP_2 binding site. From their model, they proposed an interaction of the polar PIP_2-head with a cluster of positive charged amino acids located in the proximal C-terminal region while the aliphatic chains of PIP_2 form hydrophobic interactions with transmembrane domains S5 and S6 of TRPV1 (Brauchi *et al.*, 2007). Overall, different models (direct and indirect) have been described for the interaction of TRPC3/6/7 channels with modulatory acting DAG and PIP_2 (Estacion *et al.*, 2004; Vazquez *et al.*, 2004; Smyth *et al.*, 2006; Nilius *et al.*, 2008).

We recently observed that hyperforin increases TRPC6-mediated non selective currents. As a non-selective cation channel, TRPC6 is permeable for sodium as well as for calcium. Thus, it triggers calcium-dependent intracellular signalling processes necessary for cell differentiation (Leuner *et al.*, 2007; Müller *et al.*, 2008). In PC12 cells, hyperforin mimics NGF-induced cellular responses involved in neurite outgrowth (Leuner *et al.*, 2007).

Hyperforin is a polyprenylated bicyclic acylphloroglucinol derivative. Extensive chemical degradation and derivatisation studies have established its cage like structure

(Beerhues, 2006). Pure hyperforin is not very stable when exposed to light and oxygen, which limits its clinical applications and further developments. This instability is due to the enolized β-dicarbonyl system present in the molecule. Several previous studies dealt with the chemical modification of its structure by acylation, alkylation, and oxidation, but not with a chemical simplification of hyperforin, to identify new stable and potent hyperforin analogues (Tada *et al.*, 1992; Verotta *et al.*, 1999; Verotta *et al.*, 2000; Verotta *et al.*, 2004). Notably, the core structure of hyperforin - the phloroglucinol - is rather stable. Based on the perspective of potential therapeutic applications, we became interested in the search of stable synthetic phloroglucinol-derivatives with pharmacological activity profiles comparable to that of hyperforin and acting as TRPC6-selective agonists.

Consequently, we selected simple 2-acylphloroglucinol- and 2,4-diacylphloro-glucinol-derivatives and tested them for their hyperforin-like bio-activities. Selection of nine compounds from phloroglucinol derivatives reported in the literature (Tada *et al.*, 1992) was conducted on the basis of our working hypothesis that the phloroglucinol moiety provides the essential pharmacophore of hyperforin and that its activity profile could be due to structural resemblances to DAG, PIP$_2$ and some poly-unsaturated free fatty acids (Fig. 1). A variety of methods were selected to cover all functional aspects of TRPC6 activation from single channel activity, Ca^{2+} imaging, and functional aspects such as neurite outgrowth and inhibition of synaptosomal uptake.

Materials and Methods

Sources and preparation of reagents

Hyperforin and all phloroglucinol derivatives tested were kindly supplied by the preclinical Research Department of Dr. Willmar Schwabe, Karlsruhe (Germany). 1-oleoyl-2-acetyl-*sn*-glycerol (OAG; Sigma-Aldrich, Taufkirchen, Germany) and phloroglucinol was used from 100 mM stock solution in dimethyl sulfoxide. NGF (Sigma-Aldrich) was dissolved in distilled water and prepared in 50 µg/ml stock solution. GdCl$_3$, LaCl$_3$ (Sigma-Aldrich) were dissolved in H$_2$O before experiments. Other chemicals were dissolved in DMSO in stock solutions, and diluted before use. For pharmacological treatments, chemicals were present throughout the experiment. ^{3}H-serotonin was obtained from BIOTREND Chemicals GmbH (Cologne, Germany) and Lumasafe scintillation cocktail from PerkinElmer (Waltham, USA). Standard laboratory chemicals were obtained from Sigma-Aldrich. The nine 2-acyl- and 2,4-diacyl-phloroglucinol derivatives used in this study (Hyp1-9) were synthesized, purified and characterized according to Tada et al. (Tada *et al.*, 1992).

Cell culture and transfection of HEK293 cells and PC12 cells

HEK293 cells were cultured in Dulbecco's modified Eagle's medium (DMEM; Invitrogen, Groningen, The Netherlands) with 10% heat-inactivated fetal calf serum (Sigma-Aldrich), 50 U/ml penicillin (Sigma-Aldrich), and 50 µg/ml streptomycin (Sigma-Aldrich) at 37 °C under a 5% CO$_2$ humidified atmosphere at 37 °C. Cells were plated in 85 mm dishes onto glass cover slips and transiently transfected 24 h later by addition of a transfection cocktail containing 0.5 to 1 µg of DNA and 1 to 2 µl of FuGENE 6 transfection reagent (Roche Diagnostics, Indianapolis, IN, USA) in 97 µl of Opti-MEM medium (Invitrogen). The cDNA constructs for TRPC3, TRPC6, and TRPC7 have been kindly provided by Dr. Michael Schaefer (20). Fluorescence measurements and electrophysiological studies were carried out 1 to 2 days after transfection. PC12 cells were cultured in DMEM supplemented with 10% heat-inactivated fetal calf serum and 5% heat-inactivated horse serum, 50 U/ml penicillin, and 50 µg/ml streptomycin at 37 °C in a humidified incubator containing 5% CO$_2$. Before Ca^{2+} imaging, cells were plated in 85 mm dishes onto glass cover slips. Transient transfection of PC12 cells was

conducted using FuGENE 6 transfection reagent (Roche Diagnostics). Cells were plated in 85 mm dishes onto glass cover slips and transiently transfected by addition of a transfection cocktail containing 0.5 to 1 µg of DNA and 2 µl of FuGENE 6 transfection reagent (Roche Diagnostics) in 97 µl of Opti-MEM medium (Invitrogen). Fluorescence measurements were conducted 2 days after transfection. Neurite outgrowth assays were conducted 3 days after transfection.

Patch clamp experiments

Membrane currents were recorded using the perforated whole-cell configuration of the patch-clamp technique at room temperature. Pipettes were made from borosilicate glass capillary tubes. The pipettes resistance was 4-5 MΩ. Currents through the pipette were recorded by an Axopatch 200B amplifier (Axon Instruments), filtered at 2 kHz (Bessel filter) and digitized at 5 kHz. Data acquisition and command potentials were controlled with commercial software programs using a CED1401 interface (Cambridge Electronic Design Limited, Cambridge, UK) or Iso2 (MFK). Whole cell currents were elicited by voltage ramps from -100 to $+100$ mV (400 ms duration) applied every 10 seconds from a holding potential of -40 mV. The standard bath solution contained 140 mM NaCl, 5 mM KCl, 2 mM $CaCl_2$, 1 mM $MgCl_2$, 10 mM glucose and 10 mM HEPES (pH 7.4 with NaOH). Pipettes were filled with a solution containing amphotericin B (250 mg/ml) in 100 mM Cs-aspartate, 40 mM CsCl, 0.4 mM $CaCl_2$, 2 mM $MgCl_2$, 1 mM EGTA and 10 mM HEPES (pH 7.2 with CsOH). Analysed data were expressed as mean ± SEM, and a paired Student t test was used for data comparison with the level of significance set at $P < 0.05$.

Fluorescence measurements

$[Ca^{2+}]_i$ measurements in single cells were carried out using the fluorescence indicator fura-2-AM in combination with a monochromator-based imaging system (T.I.L.L. Photonics, Martinsried, Germany, or Attofluor Ratio Vision system) attached to an inverted microscope (Axiovert 100, Carl Zeiss, Oberkochen, Germany). HEK293 cells and PC12 cells were loaded with 4 µM fura-2-AM (Invitrogen) and 0.01% Pluronic F-127 (Invitrogen) for 45 min at room temperature in a standard solution composed of

8

138 mM NaCl, 6 mM KCl, 1 mM MgCl$_2$, 2 mM CaCl$_2$, 5.5 mM glucose, and 10 mM HEPES (adjusted to pH 7.4 with NaOH). Cover slips were then washed in this buffer for 20 min and mounted in a perfusion chamber on the microscope stage. For [Ca^{2+}]$_i$ measurements, fluorescence was excited at 340 and 380 nm. After correction for background fluorescence, the fluorescence ratio $F$340/$F$380 was calculated. For [Ba^{2+}]$_i$ and [Sr^{2+}]$_I$ cells were washed three times following incubation with Ca^{2+}-free standard solution. The influx of Ba^{2+} and Sr^{2+} was evaluated in fura-2-loaded cells by measuring the fluorescence of Ba^{2+} or Sr^{2+} fura-complexes.

Synaptosomal serotonin uptake

For neurotransmitter uptake experiments synaptosomal preparations were obtained from whole brain of female 2 – 3 month old mice. The tissue was homogenized in ice-cold sucrose solution (0.32 M) and diluted with 10 ml of the homogenizing medium. The nuclear fraction was eliminated by centrifugation at 750 g for 10 min (Beckman Centrifuge, Model J2– 21; Beckman Coulter, Fullerton, CA). The supernatant was centrifuged at 17.400 g for 20 min to obtain the crude synaptosomal pellets. The pellets were suspended in 11 ml of ice-cold Krebs-HEPES-buffer (150 mM NaCl, 10 mM HEPES, 6.2 mM KCl, 1.2 mM Na$_2$HPO4, 1.2 mM MgSO4, 10 mM glucose, 10 mM pargyline, and 0.1% ascorbic acid; pH 7.4 at 37 °C), aliquoted in microtiter plates, incubated in the presence of varying concentrations of the drugs tested at 37 °C for 15 min in a shaking water bath, and cooled on ice. 2.9 nM ^{3}H-serotonin was added and the uptake experiment started by incubation at 37 °C for 4 min. The probes were cooled, immediately filtered through Whatman GF/B glass fiber filters, and washed three times with ice-cold buffer solution with a Brandel cell harvester. Filters were placed in plastic scintillation vials containing 4 ml of Lumasafe scintillation cocktail (Packard, Meriden, CT). Radioactivity was measured after 12 h. Non-specific uptake was determined in parallel probes maintained throughout on ice or containing unlabeled serotonin (1 mM serotonin).

Neurite outgrowth of PC12 cells

Cells were plated at a density of 9 cells/plate (85 mm, polylysin coated) in 15% serum containing medium overnight. The next day, medium was changed to a medium containing 2% serum and NGF (50 ng/ml), hyperforin, the 2,4-diacylphloroglucinols or hyperforin and 2,4-diacylphloroglucinols supplemented with La^{3+} or Gd^{3+}. The neurite length was examined 3 days after different treatment regimes. After 3 days PC12 cells were fixed with paraformaldehyde solution (4%) and stained with Mayer's hematoxylin & eosin solutions. 10 cells from each stain ($n = 1$) were arbitrarily investigated and neurite length was detected by using Nikon NIS Elements AR 2.1 software.

Pharmacophore alignment

Based on the crystal structure of of hyperforin in complex with the pregnan X receptor (Protein Data Bank identifier PDB 1m13 (Watkins *et al*., 2003), resolution 2.15 Å) all atoms involved in hydrogen bridges were classified as hydrogen bond donors or acceptors, and the core as hydrophobic. Three of four hydrogen bonds were regarded as essential (interaction with Ser247, His407, Gln285), the forth to a water molecule as optional, since water molecules cannot be expected at similar positions in TRPC6. Flexible pharmacophore-based alignments were performed with the software MOE (version 2008.9, Chemical Computing Group, 1010 Sherbrooke St. W, Suite 910, Montreal, Quebec, Canada H3A 2R7). The minimal number of matched features was set to three. For depiction of results we used Pymol version 1.0 (www.pymol.org, Copyright © 2008 DeLano Scientific LLC). .

Results

Inhibition of serotonin uptake

Several phloroglucinol derivatives were selected to investigate our working hypothesis that the phloroglucinol moiety of hyperforin represents its essential pharmacophore, and that its structural resemblance to DAG, PIP_2 and PUFAs might explain its observed activity profile. We first tested the effects of phloroglucinol, DAG, and several 2-acyl-, and 2,4-diacylphloroglucinols on serotonin uptake (Fig. 1). Subsequently, we determined the IC_{50} values of the selected substances in comparative experiments with hyperforin. The ^{3}[H]-serotonin uptake in murine synaptosomes was inhibited by hyperforin with an IC_{50} value of 1.93 µM (Fig. 2A), whereas the uptake was blocked by Hyp9 with an IC_{50} value of 11.1 µM (Fig. 2B). To further analyse the functional capability of the selected derivatives, we compared the inhibitory effect at a single concentration (Fig. 2C; 10 µM). Like hyperforin, and the endogenous activator of TRPC6 DOG (100 µM), Hyp1, Hyp5, Hyp7, Hyp8 and Hyp9 inhibited serotonin uptake in murine synaptosomes with comparable IC_{50} values ranging from 1.5 µM for Hyp7 to 11.1 µM for Hyp9 (Fig. 2D). Phloroglucinol, Hyp2, Hyp3, Hyp4, and Hyp6 failed to inhibit serotonin uptake. These data clearly suggested that 2,4-diacylphloroglucinol structures can mimic hyperforin-mediated effects, and that they could represent represents a novel class of easily accessible the pharmacophore.

2,4-Diacylphloroglucinols induce neurite outgrowth

TRPC6 channels are highly expressed in the brain and are involved in local processes such as growth cone turning, neurite extension, the formation of excitatory synapses and in spatial learning and memory (Li *et al.*, 2005; Tai *et al.*, 2008). Previously, we have shown that hyperforin is able to induce neurite outgrowth in PC12 cells at clinically relevant concentrations of 0.3 µM (Leuner *et al.*, 2007). Therefore, we investigated the effects of phloroglucinol and all phloroglucinol derivatives on neurite outgrowth. PC12 cells were incubated for 3 days with 0.3 µM phloroglucinol, or hyperforin, or the derivatives, or 50 ng/µl NGF. Differentiation of PC12 cells was determined by measuring neurite lengths in PC12 cells after three consecutive days of treatment. Hyp1, Hyp5, Hyp7, Hyp8 and Hyp9 induced neurite outgrowth comparable

with the effect induced by hyperforin or NGF (Fig. 3A, and B). Phloroglucinol and Hyp2, Hyp3, Hyp4, and Hyp6 were ineffective.

Since, we previously showed that the induction of neurite outgrowth is mediated by TRPC6 channels, we next tested the role of these channels to further characterize the pharmacological profile of the new structures. We used pharmacological and genetic approaches to interfere with TRPC6 activity. First, PC12 cells were incubated with the TRP channel blockers lanthanum (100 µM) and gadolinium (100 µM) ions in the presence of the active phloroglucinol derivatives. The neurite outgrowth induced by Hyp1, Hyp5, Hyp7, Hyp8 and Hyp9 was dramatically reduced by the co-incubation with gadolinium and lanthanum (Fig. 3C). These results are consistent with TRPC6 mediated effects. This presumption was further validated by a genetic approach using a dominant-negative TRPC6 mutant. We transiently transfected PC12 cells with TRPC6-DN-YFP and incubated the transfected cell for two days in the presence of the active phloroglucinol derivatives. In TRPC6-DN-YFP expressing cells, the Hyp1-, Hyp5-, Hyp7-, Hyp8- and Hyp9-induced outgrowth of neurites were completely abolished, which strongly argues for the involvement of TRPC6 channels in the 2,4-diacylphloroglucinol-induced neurite outgrowth.

Symmetric 2,4-diacylphloroglucinols induce non-selective cation influx in PC12 cells

In order to provide further evidence that 2,4-diaclyphloroglucinol represent the active core of hyperforin pharmacophore, we studied Ca^{2+} and Ba^{2+} fluxes by imaging techniques using the intracellular calcium indicator fura-2. The experimental set-up was comparable to the approaches described before. Hyperforin and the phloroglucinol structures were applied at concentrations of 10 µM to fura-2-loaded PC12 cells. Hyp1, Hyp5, Hyp7, Hyp8 and Hyp9 induced a robust and transient elevation of $[Ca^{2+}]_i$, which is comparable to hyperforin (Fig. 4A, and C). Hyp2, Hyp3, Hyp4, and Hyp6 failed to increase $[Ca^{2+}]_i$ (Fig. 4B and C). EC_{50} values determined for the active compounds were comparable to that of hyperforin, and ranged from 1.26 µM for Hyp9 to 7.17 for Hyp8. In addition, the measurements of Ba^{2+} entry showed a comparable profile of the test compounds (Fig. 4E). Transfection of PC12 cells with the dominant-negative TRPC6 construct prior to fura-2-loading of the cells diminished the stimulatory effect of the 2,4-

diacylphloroglucinols (Fig. 4F). To finally complete the pharmacological profile of the 2,4-diaclyphloroglucinols, we used gadolinium (100 µM) and lanthanum ions (100 µM), SK&F 96365 (10 µM), N-(p-amylcinnamoyl)anthranilic acid (ACA; 30 µM), and 2-aminophenoxyborate (2-APB; 30 µM) known to interfere with non-selective cation channels especially TRPC channels (Fig. 4G). As the profile of the compounds strongly argued for the involvement of TRP channels in the derivative-induced Ca^{2+} influx, we also tested ruthenium red (RR) (10 µM), which blocks TRPV, TRPM6, TRPM8 and TRPA1 channels (Leuner *et al.*, 2007). RR had no effect on hyperforin-induced calcium entry and thereby allowed to narrow down the variety of putative candidates mainly to TRPC channels. The results are summarized in Figure 4G and consistent with the idea that 2,4-diacylphoroglucinols represent the pharmacophore of hyperforin.

TRPC6-mediated currents are induced by 2,4-(1-keto-hexyl) phloroglucinol (HYP9)

Based on the *EC₅₀* values determined for the active 2,4-diacylphoroglucinol derivatives (Fig. 4D), we choose the most potent structure for electrophysiological characterization in whole-cell patch clamp experiments. As shown in Figure 5, Hyp9 (10 µM) markedly stimulated whole-cell currents in TRPC6-expressing HEK293 cells (Fig. 5A, B). Mean current densities at +90 mV and –90 mV measured after 3-5 minutes of application of Hyp9 were significantly increased in TRPC6 transfected cells (Fig. 5B). The current increase was blocked by subsequent application of Gd^{3+} (100 µM). Thus, these effects were similar compared to the effects of hyperforin on recombinant TRPC6 channels in HEK293 cells (Leuner *et al.*, 2007).

In addition to recombinantly expressed TRPC6 channels in HEK293 cells, we studied the activation of natively expressed TRPC6-like channels by hyperforin and Hyp9 in PC12 cells, the cell model also used for experiments testing the capability of hyperforin and the Hyp-derivatives to enhance neurite outgrowth. Whole-cell patch clamp experiments were performed in the absence (Fig. 5C, D) and presence of gadolinium ions (100 µM) (Fig. 5E, F). Hyperforin (10 µM, Fig. 5C) and Hyp9 (10 µM, Fig. 5D) induced similar inward and outward currents over time. Upon application, currents developed over time with maximal current amplitudes after 5 min. In the presence of Gd^{3+} (100 µM) neither hyperforin- nor Hyp9-induced currents were

13

detectable (Fig. 5 E, F). The current-voltage-relationships of both hyperforin- and hyp9-induced currents in PC12 cells elicited by voltage ramps were almost linear and comparable with values shown for currents recorded from recombinantly expressed TRPC6.

2,4-Diacylphloroglucinols selectively activate TRPC6

Diacylglycerol activates TRPC3, TRPC6, and TRPC7, whereas hyperforin selectively stimulates only TRPC6. We next studied the central question, whether the pronounced TRPC6 selectivity of 2,4-diacylphloroglucinol derivatives has been conserved or lost by these compounds. Therefore, we transiently expressed TRPC3, TRPC6 and TRPC7 protein as YFP fusion proteins in HEK293 cells (Fig. 6). The functional expression was verified by the application of OAG (100 µM) prior to the addition of hyperforin (10 µM) (Fig. 6A) and Hyp5 (Fig. 6B). In both experimental configurations, the substances induced transient effects in TRPC6-expressing cells, whereas the fluorescence remained unchanged in TRPC3- and TRPC7-expressing cells. The statistical analysis of these experiments is given in Figure 6C to E. The data show that the 2,4-diacylphloroglucinol derivative carry not only the active moiety of hyperforin but also the selectivity to TRPC6. Based on the different experimental data, we started with structure-activity-relation (SAR) evaluations in order to see if a binding-site for the known stimulating drugs can be extracted.

Predicted ligand binding modes for hyperforin, DAG and the phloroglucinol derivatives

Due to the fact that an experimentally determined three-dimensional structure of the DAG or hyperforin binding pocket in TRPC6 is unavailable, we analysed the hyperforin derivatives and DAG regarding their possible binding conformation using the complex of pregnane X receptor and hyperforin as a reference (Watkins *et al.*, 2003). As PXR binds hyperforin in a supposedly bioactive form, we used this complex to define potential pharmacophoric points for the interaction to TRPC6. The bound hyperforin conformation provided detailed information about essential interaction points and was

adapted for prediction and evaluation of hyperforin and phloroglucinol derivatives and their substructural features.

By applying modelling techniques (Jones *et al.*, 1995; Lovell *et al.*, 2003) for automated molecular docking we could define a common binding mode for hyperforin and DAG, the putative endogenous ligand. We selected three amino acids as essential for binding from the receptor site of PXR and designed a procedure to test the hypothesis that hyperforin derivatives show similar interactions which might also be present in TRPC6. We focused on Hyp2 and on Hyp7. Prediction of possible binding modes for TRPC6 binding ligands was performed with two modelling approaches including molecular docking and pharmacophore alignment.

Initially, DAG was docked into the PXR receptor, so that three oxygens could be predicted to interact with similar residues as hyperforin (Fig. 7). The docking procedure constrained the hydrogen bonds to the same protein protonation state as observed for hyperforin and PXR. However, docking of synthesised phloroglucinol derivatives did not allow for the discrimination between the 'up' and 'down' orientation of the ligand in the binding pocket (Fig. 8B), but suggests an interaction to identical side chains regardless of the ligand orientation. Thus, pharmacophore alignment was applied and the result was in agreement with the 'down' conformation of the ligand (Fig. 8A).

The 'down' conformation is in better agreement with experimental findings, which suggest that both carbonyl groups of the derivates are essential for activity: ligand derivatives lacking a second carbonyl function were inactive in activity assays (*e.g.*, Hyp3).

Discussion

Starting with the challenging job of the development of stable phloroglucinol derivatives carrying the pharmacological properties of hyperforin, we finally identified five 2,4-diacylphloroglucinol derivative meeting the initial demand. By extensive pharmacological characterisation, including transmitter uptake, neurite outgrowth, calcium imaging assays, electrophysiological recordings, and modelling approaches, we identified symmetric 2,4-diacylphloroglucinol derivatives as potent and selective hyperforin-like TRPC6 activators.

We tested our working hypothesis that the phloroglucinol moiety of hyperforin represents the essential pharmacophore and reflects structural resemblance to DAG, PIP_2, and PUFAs might be important for activity. Importantly, phloroglucinol itself failed to inhibit serotonin uptake and activate TRPC6 channels. Only the symmetric 2,4-diacylphloroglucinol derivatives which possess acyl chains composed of 1 – 5 carbons or acyl chains composed of 1 – 2 carbons substituted with a benzene ring led to a pronounced activation of TRPC6 channels. To our surprise, long aliphatic side chains observed in Hyp3 with 15 carbons did not activate TRPC6 channels. In addition, non-symmetric 2-acylphloroglucinol derivatives like Hyp2 or Hyp6 showed no effect on TRPC6 channels. Methylation of one the hydroxyl functions of phloroglucinol moiety in Hyp1 also resulted in an inactive compound (Hyp4). In previous studies, hyperforin was modified by acylation, alkylation, and oxidation leading to a series of hyperforin analogues which were subsequently used to study structure–activity relationships (Verotta *et al.*, 2002). All these compounds were less potent inhibitors of synaptosomal serotonin reuptake than the parental compound, indicating a specific role for the enolized beta-diketone moiety. The same was true for the synthesized phloroglucinols examined, suggesting that a covalent block of the tautomeric equilibrium by oxidation is detrimental for pharmacological activity.

Our modelling studies of possible ligand binding modes suggest that hyperforin, DAG, and the active hyperforin like phloroglucinol derivatives have similar pharmacophoric characteristics. The definition of these interactions originated form a crystal structure of PXR in complex with hyperforin and provided the basis for prediction of a probable three-dimensional conformation of the ligands, which would satisfy

comparable hydrogen bonds as observed in the complex structure. The computed preferred 'down' conformation of hyperforin and the active derivatives is supported by our experimental findings and indicates that both carbonyl groups of the derivates are essential for activity. This binding mode could also explain the inactivity of Hyp2 and Hyp6. The selectivity of hyperforin and the symmetric 2,4-diacylphloroglucinols for TRPC6 might be due to the rigid structure of these compounds. In contrast, DAG is more flexible and might be able to interact with amino acids that are placed differently in TRPC3 and TRPC7 channels. The putative TRPC6 docking site of hyperforin in comparison to the PXR binding pocket will support further steps in compound optimisation.

In summary, several symmetric 2,4-diacylphloroglucinol derivatives are the first chemically simplified and stable molecules, which share the pharmacological profile with hyperforin and are potent and selective TRPC6 activators. Based on the profile of the tested TRP channels, we currently can not exclude the possibility that hyperforin or the 2,4-diacylphoroglucinol derivatives are modulators of unknown nonselective cation channels. In contrast to previous studies which modified the complex hyperforin structure, *e.g.* by alkylation or oxidation, we were able to create simplified chemical lead structures with 2,4-diacylphoroglucinol moiety as the essential pharmacophore. This structural core is essential for activation of TRPC6 channels which indirectly results in the inhibition of neurotransmitter uptake as well as to stimulation of neuronal differentiation processes. Our modelling studies suggest that the natural TRPC6 activator DAG, hyperforin, and the symmetric 2,4-diacylphloroglucinol derivatives share common interaction points with the target protein. Further evaluation of the crystal structure of TRPC6, and the identification of the binding pocket of hyperforin or other endogenous ligands is urgently needed to provide more insight into the structure-activity relationship of phloroglucinol derivates.

Acknowledgements

MOL # 57513

References

Beerhues L (2006) Hyperforin. *Phytochemistry* **67**: 2201-2207.

Brauchi S, Orta G, Mascayano C, Salazar M, Raddatz N, Urbina H, Rosenmann E, Gonzalez-Nilo F and Latorre R (2007) Dissection of the Components for PIP2 Activation and Thermosensation in TRP Channels. *Proc Natl Acad Sci U S A* **104**: 10246-10251.

Dietrich A and Gudermann T (2007) TRPC6. *Handb Exp Pharmacol* **179**: 125-141. Springer Verlag, Berlin

Estacion M, Li S, Sinkins W G, Gosling M, Bahra P, Poll C, Westwick J and Schilling W P (2004) Activation of Human TRPC6 Channels by Receptor Stimulation. *J Biol Chem* **279**: 22047-22056.

Hofmann T, Obukhov A G, Schaefer M, Harteneck C, Gudermann T and Schultz G (1999) Direct Activation of Human TRPC6 and TRPC3 Channels by Diacylglycerol. *Nature* **397**: 259-263.

Jardin I, Redondo P C, Salido G M and Rosado J A (2008) Phosphatidylinositol 4,5-Bisphosphate Enhances Store-Operated Calcium Entry Through HTRPC6 Channel in Human Platelets. *Biochim Biophys Acta* **1783**: 84-97.

Jia YC, Zhou J, Tai Y L and Wang Y Z (2007) TRPC Channels Promote Cerebellar Granule Neuron Survival. *Nat Neurosci* **10**: 559-567.

Jones G, Willett P and Glen R C (1995) Molecular Recognition of Receptor-Sites Using A Genetic Algorithm With A Description of Desolvation. *J Mol Biol* **245**: 43-53.

Kwon Y, Hofmann T and Montell C (2007) Integration of Phosphoinositide- and Calmodulin-Mediated Regulation of TRPC6. *Mol Cell* **25**: 491-503.

Lemonnier L, Trebak M and Putney J W (2008) Complex Regulation of the TRPC3, 6 and 7 Channel Subfamily by Diacylglycerol and Phosphatidylinositol-4,5-Bisphosphate. *Cell Calcium* **43**: 506-514.

Leuner K, Kazanski V, Müller M, Essin K, Henke B, Gollasch M, Harteneck C and Müller W E (2007) Hyperforin a Key Constituent of St. John's Wort Specifically Activates TRPC6 Channels. *FASEB J* **21**: 4101-4111.

Li Y, Jia Y C, Cui K, Li N, Zheng Z Y, Wang Y Z and Yuan X B (2005) Essential Role of TRPC Channels in the Guidance of Nerve Growth Cones by Brain-Derived Neurotrophic Factor. *Nature* **434**: 894-898.

Linde K, Berner M M and Kriston L (2008) St John's Wort for Major Depression. *Cochrane Database Syst Rev*. **4**: CD000448

Lovell SC, Davis I W, Adrendall W B, de Bakker P I W, Word J M, Prisant M G, Richardson J S and Richardson D C (2003) Structure Validation by C Alpha Geometry: Phi,Psi and C Beta Deviation. *Proteins* **50**: 437-450.

Mandadi S and Roufogalis B D (2008) ThermoTRP Channels in Nociceptors: Taking a Lead From Capsaicin Receptor TRPV1. *Curr Neuropharmacol* **6**: 21-38.

Montell C (2005) The TRP Superfamily of Cation Channels. *Sci STKE* **272**: re3.

Montell C (2006) TRP Channels: Mediators of Sensory Signaling and Roles in Health and Disease. *Chem Senses* **31**: A45.

Müller M, Hill K, Beschmann H, Rubant S, Boehncke W H, Harteneck C, Müller W E and Leuner K (2008) Specific TRPC6 Channel Activation, a Novel Approach to Stimulate Keratinocyte Differentiation. *J Biol Chem* **283**: 33942-54.

Müller WE (2003) Current St John's Wort Research From Mode of Action to Clinical Efficacy. *Pharmacol Res* **47**: 101-109.

Nilius B, Owsianik G and Voets T (2008) Transient Receptor Potential Channels Meet Phosphoinositides. *Embo Journal* **27**: 2809-2816.

Singer A, Wonnemann M and Müller W E (1999) Hyperforin, a Major Antidepressant Constituent of St. John's Wort, Inhibits Serotonin Uptake by Elevating Free Intracellular Na$^+$. *J Pharmacol Exp Ther* **290**: 1363-1368.

Smyth JT, Lemonnier L, Vazquez G, Bird G S and Putney J W (2006) Dissociation of Regulated Trafficking of TRPC3 Channels to the Plasma Membrane From Their Activation by Phospholipase C. *J Biol Chem* **281**: 11712-11720.

Tada M, Chiba K, Takakuwa T and Kojima E (1992) Analogs of Natural Phloroglucinols As Antagonists Against Both Thromboxane-A2 and Leukotriene-D4. *J Med Chem* **35**: 1209-1212.

Tai Y, Feng S, Ge R, Du W, Zhang X, He Z and Wang Y (2008) TRPC6 Channels Promote Dendritic Growth Via the CaMKIV-CREB Pathway. *J Cell Sci* **121**: 2304-7.

Trebak M, St J B, McKay R R, Birnbaumer L and Putney J W, Jr. (2003) Signaling Mechanism for Receptor-Activated Canonical Transient Receptor Potential 3 (TRPC3) Channels. *J Biol Chem* **278**: 16244-16252.

Treiber K, Singer A, Henke B and Müller W E (2005) Hyperforin Activates Nonselective Cation Channels (NSCCs). *Br J Pharmacol* **145**: 75-83.

Vazquez G, Wedel B J, Kawasaki B T, Bird G S and Putney J W (2004) Obligatory Role of Src Kinase in the Signaling Mechanism for TRPC3 Cation Channels. *J Biol Chem* **279**: 40521-40528.

Verotta L, Appendino G, Belloro E, Bianchi F, Sterner O, Lovati M and Bombardelli E (2002) Synthesis and Biological Evaluation of Hyperforin Analogues. Part I. Modification of the Enolized Cyclohexanedione Moiety. *J Nat Prod* **65**: 433-438.

Verotta L, Appendino G, Belloro E, Jakupovic J and Bombardelli E (1999) Furohyperforin, a Prenylated Phloroglucinol From St. John's Wort (Hypericumperforatum). *J Nat Prod* **62**: 770-772.

Verotta L, Appendino G, Jakupovic J and Bombardelli E (2000) Hyperforin Analogues From St. John's Wort (Hypericum Perforatum). *J Nat Prod* **63**: 412-415.

Verotta L, Lovaglio E, Sterner O, Appendino G and Bombardelli E (2004) Modulation of Chemoselectivity by Protein Additives. Remarkable Effects in the Oxidation of Hyperforin. *J Org Chem* **69**: 7869-7874.

Voets T and Nilius B (2007) Modulation of TRPs by PIPs. *J Physiol* **582**: 939-944.

Voets T, Talavera K, Owsianik G and Nilius B (2005) Sensing With TRP Channels. *Nat Chem Biol* **1**: 85-92.

Watkins RE, Maglich J M, Moore L B, Wisely G B, Noble S M, Davis-Searles P R, Lambert M H, Kliewer S A and Redinbo M R (2003) 2.1 A Crystal Structure of Human PXR in Complex With the St. John's Wort Compound Hyperforin. *Biochemistry* **42**: 1430-1438.

Wonnemann M, Singer A and Müller W E (2000) Inhibition of Synaptosomal Uptake of ^{3}H-L-Glutamate and 3H-GABA by Hyperforin, a Major Constituent of St. John's Wort: the Role of Amiloride Sensitive Sodium Conductive Pathways. *Neuropsychopharmacology* **23**: 188-197.

Zhou J, Du W, Zhou K, Tai Y, Yao H, Jia Y, Ding Y and Wang Y (2008) Critical Role of TRPC6 Channels in the Formation of Excitatory Synapses. *Nat Neurosci* **11**: 741-743.

MOL # 57513

Footnotes:

[*] both authors are contributed equally

Legends for figures

Fig. 1: Structures of hyperforin, DAG, PIP$_2$ phloroglucinol and phloroglucinol derivatives tested.

Fig. 2: Effects of hyperforin, phloroglucinol and its derivatives on serotonin uptake in murine synaptosomes Serotonin uptake was measured using ^{3}H serotonin in murine synaptosomes. The synaptosomes were preincubated for 15 min with varying concentrations of hyperforin, phloroglucinol and its derivatives. Concentration-response curves are shown for the inhibition of ^{3}H-Serotonin uptake by hyperforin (*A*) and by Hyp9 (*B*). Summary of the effects of the hyperforin, phloroglucinol, and the different hyperforin derivatives at a concentration of 10 µM on serotonin uptake (C). The IC$_{50}$ values obtained for the phloroglucinol derivatives and phloroglucinol are compared with the IC$_{50}$ of hyperforin (D; Error bars indicate ± SEM; n = 6).

Fig. 3: Phloroglucinol derivatives induce neurite outgrowth in PC12 cells via TRPC6 activation. Neurite outgrowth assays were performed using PC12 cells. *A*) PC12 cells were treated with NGF (50 ng/ml), hyperforin, phloroglucinol and hyperforin derivatives (0.3 µM) for 3 consecutive days. After a 3 day incubation period the average neurite extension was measured and the data of treated cells were compared to NGF-stimulated PC12 cells. Hyp1, Hyp5, Hyp7, Hyp8, and Hyp9 induced a significant neurite outgrowth (Error bars indicate ± SEM; n = 6; unpaired t-test, p < 0.01). *B)* Representative images of PC12 cells with neurite extensions are shown from experiments after a 3 day incubation period in untreated control cells, in cells in the presence of NGF (50 ng/ml), hyperforin (0.3 µM), Hyp2 (0.3 µM), Hyp5 (0.3 µM), and Hyp9 (0.3 µM; *n* = 6). *C)* Neurite extension induced by hyperforin or the active phloroglucinol derivatives was measured in the presence and absence of La^{3+} (100 µM) or Gd^{3+} (100 µM) for 5 days. Results are expressed as % of the neurite length average in the absence of the TRP channel blockers. Both inhibitors blocked the effect of Hyp1, Hyp5, Hyp7, Hyp8, and Hyp9 significantly (Error bars indicate ± SEM; n = 6; unpaired t-test, p < 0.001). *D)* TRPC6-DN-YFP-expressing and untransfected PC12 cells were treated with hyperforin (0.3 µM) and the active phloroglucinol derivatives 24 h after transfection and differentiated over 3

consecutive days. Representative images were taken and neurite lengths were measured. The data given in the bars compare neurite outgrowth in TRPC6-DN-YFP-expressing and untransfected PC12 cells under the treatment with hyperforin and the respective derivatives. *E*) Representative images of PC12 cells expressing TRPC6-DN-YFP treated with hyperforin (0.3 µM), Hyp5 (0.3 µM), or Hyp9 (0.3 µM; $n = 3$, Error bars indicate SEM, unpaired t-test, *p < 0.05, **p < 0.01, ***p < 0.001).

Fig. 4: Phloroglucinol derivatives induce a non-selective cation influx in PC12 cells via TRPC6.

Hyperforin and phloroglucinol derivative-induced changes in $[Ca^{2+}]_i$ were characterized in fura-2-loaded PC12 cells in video-imaging experiments as described in Materials and Methods. A) Representative time traces show hyperforin and Hyp1-, Hyp5-, Hyp7-, Hyp8- and Hyp9-induced elevation of $[Ca^{2+}]_i$ (10 µM; n = 6). *B)* Representative traces from experiments using hyperforin, phloroglucinol, Hyp2, Hyp3, Hyp4, and Hyp 6 are given (10 µM; n = 6). *C)* Summarized effects of hyperforin-, phloroglucinol and the phloroglucinol derivatives (10 µM) on intracellular Ca^{2+}-concentrations in PC12 cells. *D)* EC_{50} values for hyperforin and the active derivatives Hyp1, Hyp5, Hyp7, Hyp8 and Hyp9 were calculated from Ca^{2+} imaging experiments. *E)* Non-selective cation influx induced by hyperforin, phloroglucinol and the different hyperforin derivatives was measured replacing $[Ca^{2+}]_{ex}$ by 2 mM Ba^{2+} using fura-2 fluorescence. To identify the molecular structure of the hyperforin derivatives-activated entry mechanism, we used a dominant negative knockdown of TRPC6 which was tagged with YFP (TRPC6-DN-YFP) (*F*) and different TRP channel blockers (*G*). *F)* Fura-2-loaded, TRPC6-DN-YFP expressing PC12 cells were stimulated with hyperforin and the active derivatives and compared with untransfected cells (Errors bars indicate ± SEM, $n = 6$, 5–10 cells/independent experiment, unpaired t-test, *p < 0.05, **p < 0.01, ***p < 0.001). The results are expressed as percent effect of the respective untransfected control treated with the different stimuli. *G)* Summary of changes in $[Ca^{2+}]_i$ in percentage induced by hyperforin and the respective derivatives in the presence of SK&F 96365 (10 µM, $n = 6$), La^{3+} (100 µM, $n = 6$), Gd^{3+} (100 µM, $n = 6$), 2-APB (30 µM, $n = 6$), ACA (30 µM, $n = 6$), and RR (1 µM) normalized on the Ca^{2+}-influx in the absence of the different blockers are

24

shown in *G*. SK&F 96365, La^{3+}, and Gd^{3+} significantly inhibited the Ca^{2+}-Influx induced by hyperforin and the different derivatives with p values smaller than 0.001. ACA, and 2-APB with p values between 0.05, and 0.01. RR showed no effect on Ca^{2+} influx (ns = not significant). (Error bars indicate ± SEM, unpaired t-test).

Fig. 5: Phloroglucinol derivatives induced TRPC6 currents.

Application of Hyp9 (10 µM) resulted in the significant increase in outward and inward currents in TRPC6-expressing HEK293 cells and PC12 cells. *A.)* Whole cell currents elicited by voltage ramps from –100 to +100 mV in TRPC6-expressing HEK293 cell from a holding potential of –40 mV in control (*Control*), after application of 10 µM Hyp9 (*Hyp9*) and 10 µM Hyp9 plus 100 µM Gd^{3+} (*Hyp9 + Gd^{3+}*). *B.)* Mean current density at +90 and –90 mV in control (*white*), after 3-5 min application of 10 µM Hyp9 (*gray*) and 10 µM Hyp9 plus 100 µM Gd^{3+} (*black*) in TRPC6-expressing cells (n = 7) (*p < 0.05*). *C-F.)* In the absence (C & D) and presence (E & F) of Gd^{3+} (100 µM), whole cell currents were recorded from PC12 cells stimulated by hyperforin (C & E) and Hyp9 (D & F). The currents measured at +90 and –90 mV are plotted over time. Shown are representative experiments (n = 4 in each group); the time scale is similar in all panels.

Fig. 6: Phloroglucinol derivatives activate TRPC6 channels.

To test if the active hyperforin derivatives are selective TRPC6 activators or also activate closely related TRPC3 or TRPC7 channels, we studied effects of the derivatives in TRPC3, TRPC6, and TRPC7-expressing HEK293 cells in single cell measurements. TRPC proteins were transiently expressed as C-terminal YFP fusion proteins in HEK293 cells. Functional expression of the proteins was monitored by application of either OAG (100 µM) before application of hyperforin or the respective derivative (10 µM). *A and B)* Single traces of changes in fluorescence were monitored from TRPC6-YFP- (red), TRPC3-YFP (black) or TRPC7-YFP-expressing HEK293 cells stimulated with hyperforin (A) or Hyp9 (B). Cells were consecutively stimulated with OAG (100 µM), hyperforin (10 µM; *n* = 6) or Hyp9 (10 µM). Hyperforin and Hyp9 only induced a significant Ca^{2+} increase in TRPC6-YFP-expressing HEK293. Only OAG induced changes in fluorescence in TRPC3-YFP-, TRPC6-YFP, and TRPC7-YFP-expressing cells. *C,D, and E)* Summary of experiments of TRPC6-YFP-, TRPC3-YFP- and TRPC7-

25

YFP-expressing HEK293 cells treated with hyperforin and all active phloroglucinol derivatives (10 µM). Exclusively in TRPC6-expressing HEK 293 cells, hyperforin and the all Hyp1, Hyp5, Hyp7, Hyp8, Hyp9 induced a significantly increased Ca^{2+} influx. Ca^{2+} elevation is expressed as percent compared to untransfected HEK293 cells (Error bars indicate ± SEM, n = 3, unpaired t-test, ***p < 0.001).

Fig. 7: Binding pocket of the human pregnane X receptor (PXR) in complex with hyperforin (PDB ID 1M13, white) and a docked conformation of DAG (blue). Shown are different views *A* and *B* of the model highlighting potentially relevant contact points. The interacting residues and both ligands are shown in stick representation (picture generated with Pymol). Hydrogen bonds are indicated by dashed lines, distances between hydrogen and their acceptor atoms are calculated in Å. Atom coordinates of Ser247 and Gln285 are identical to the PXR structure. The position of hydrogen from Ser247 binding to DAG were changed during docking to optimize hydrogen bond geometry, therefore both hydrogen positions are visualized.

Fig. 8: Crystal structure of human pregnane X receptor binding domain in complex with hyperforin, Hyp1, and Hyp7. Crystal structure of the human Pregane X receptor binding domain in complex with hyperforin (PDB ID 1M13, white) and an aligned conformation (flexible pharmacophore alignment) of Hyp1 (blue) (*A*). Docking conformation proposed for Hyp1 (dark blue, 'down') and Hyp7 (light blue, 'up') (*B*). Interacting residues and both ligands are shown in stick representation (picture generated with Pymol). Hydrogen bonds are indicated by dashed lines, distances between hydrogen bond donor and acceptor atoms are calculated in Å.
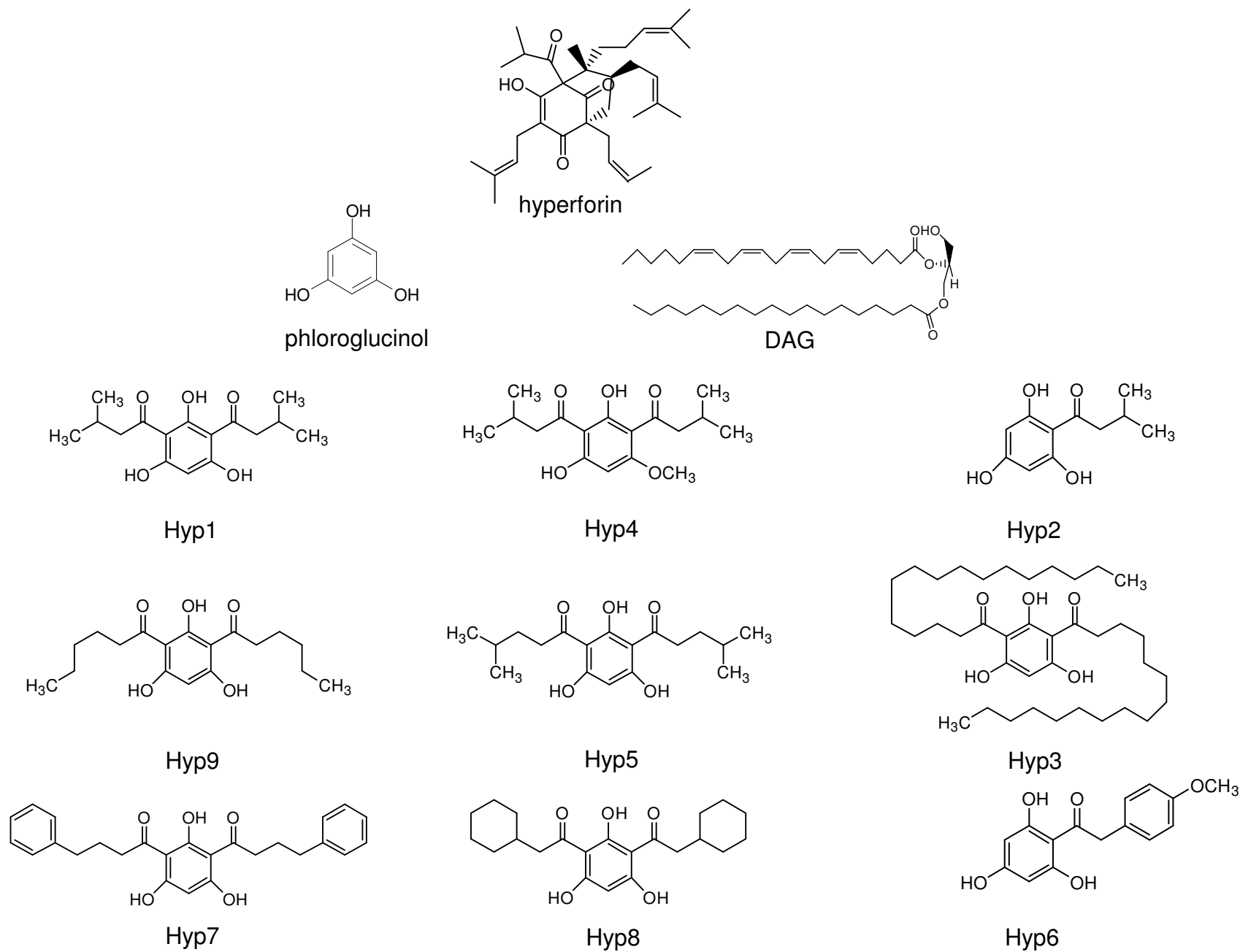
Figure 1

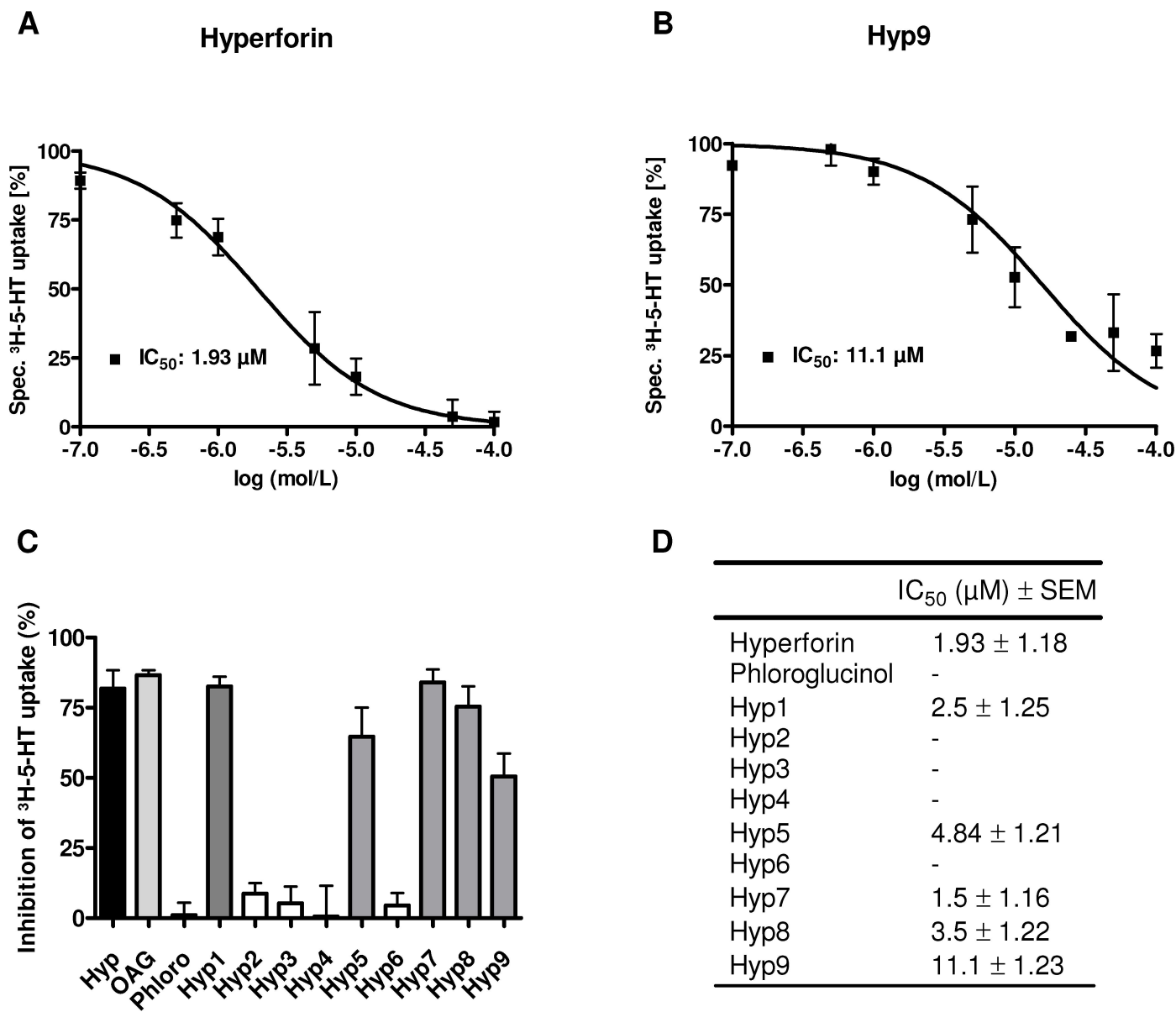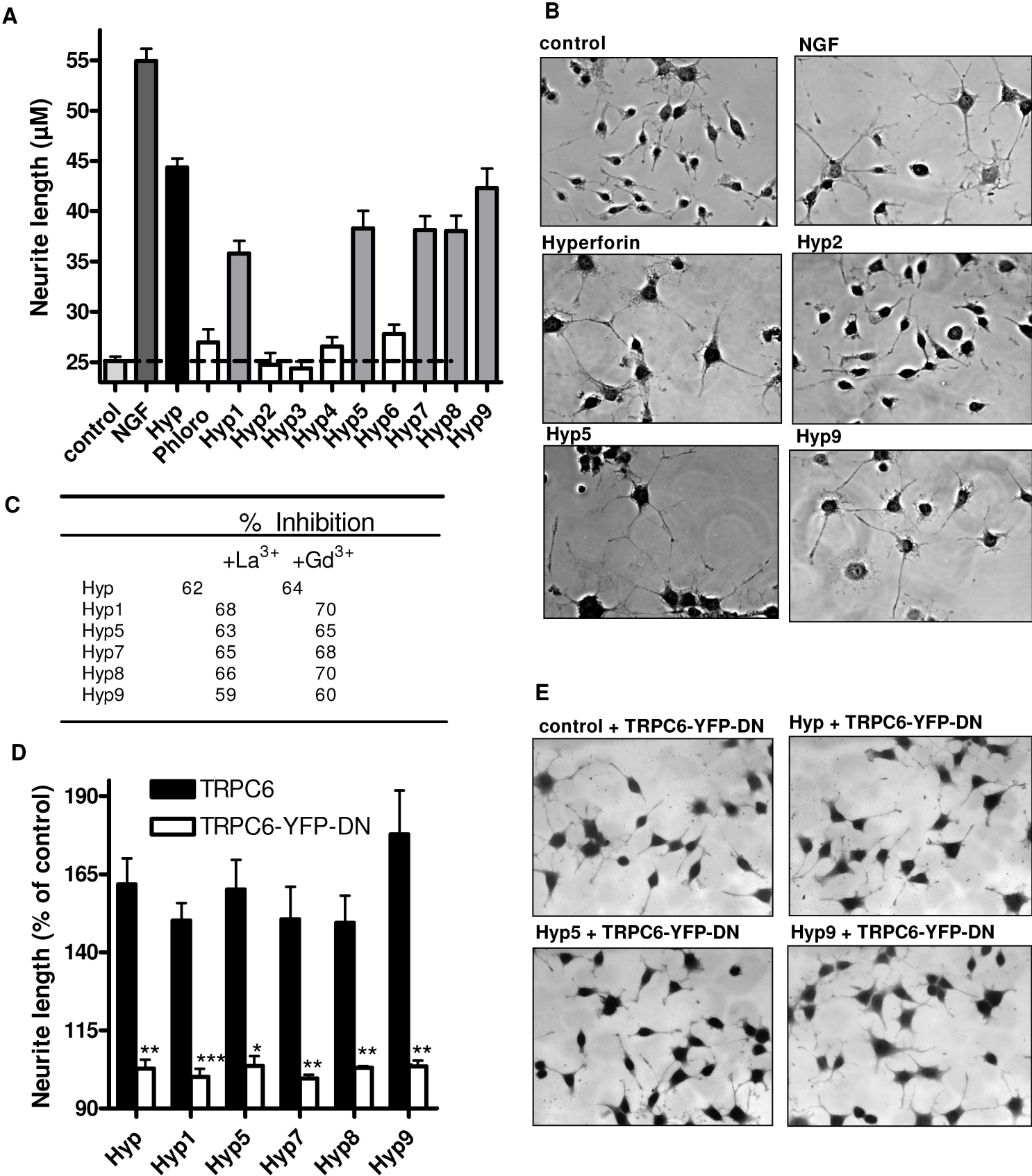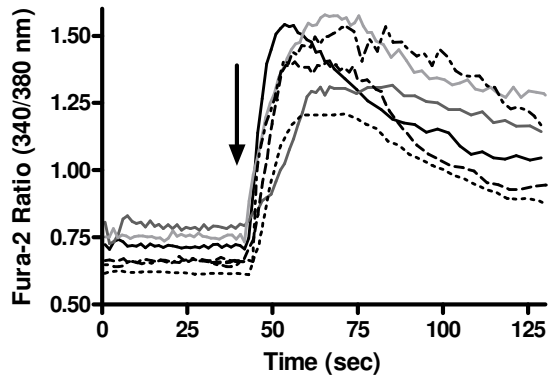hyperforin

phloroglucinol

DAG

Hyp1

Hyp4

Hyp2

Hyp9

Hyp5

Hyp3

Hyp7

Hyp8

Hyp6

Figure 2

A **Hyperforin**

IC$_{50}$: 1.93 µM

B **Hyp9**

IC$_{50}$: 11.1 µM

C

D

	IC$_{50}$ (µM) ± SEM
Hyperforin	1.93 ± 1.18
Phloroglucinol	-
Hyp1	2.5 ± 1.25
Hyp2	-
Hyp3	-
Hyp4	-
Hyp5	4.84 ± 1.21
Hyp6	-
Hyp7	1.5 ± 1.16
Hyp8	3.5 ± 1.22
Hyp9	11.1 ± 1.23

Figure 3

A

B

control   NGF

Hyperforin   Hyp2

Hyp5   Hyp9

C

	% Inhibition	
	+La^{3+}	+Gd^{3+}
Hyp	62	64
Hyp1	68	70
Hyp5	63	65
Hyp7	65	68
Hyp8	66	70
Hyp9	59	60

D

E

control + TRPC6-YFP-DN   Hyp + TRPC6-YFP-DN

Hyp5 + TRPC6-YFP-DN   Hyp9 + TRPC6-YFP-DN

Figure 4

A

B

C

D

	EC$_{50}$ (µM)
Hyperforin	1.51
Hyp1	2.71
Hyp5	1.66
Hyp7	6.35
Hyp8	7.17
Hyp9	1.26

E

Barium-Influx
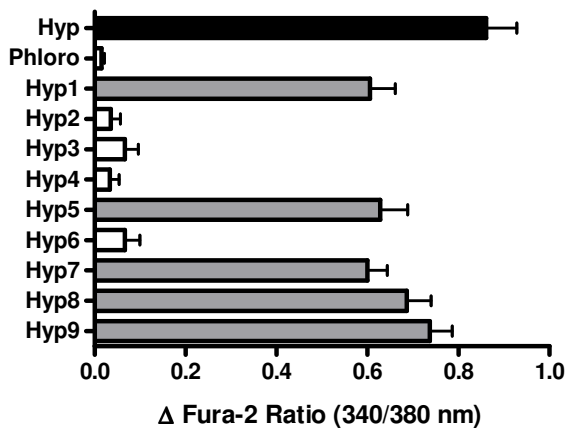
F

TRPC6-YFP-DN
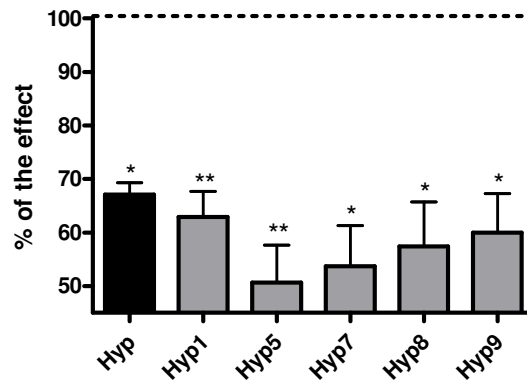
G

	% Inhibition of Ca^{2+}-Influx					
	+ La^{3+} (100 µM)	+ Gd^{3+} (100 µM)	+ SK&F (10 µM)	+ RR (1 µM)	+ ACA (30 µM)	+ 2-APB (30 µM)
Hyperforin	64	74	80	ns	35	63
Hyp1	51	65	61	ns	55	47
Hyp5	64	64	64	ns	37	48
Hyp7	62	68	62	ns	46	63
Hyp8	55	63	48	ns	54	71
Hyp9	57	64	62	ns	35	41

Figure 5
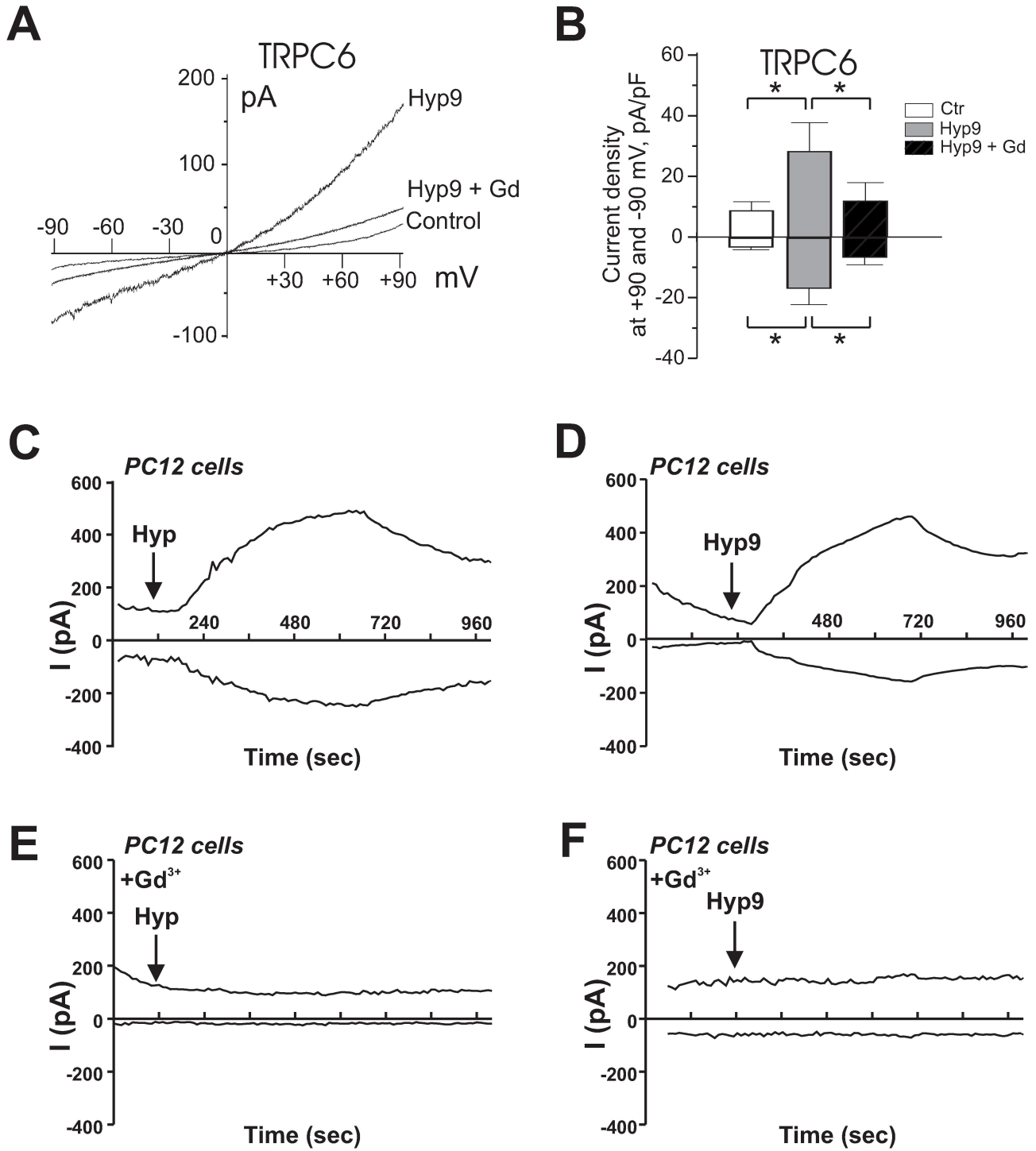
Figure 6

Figure 7

Figure 8